Visualizing Embolism Propagation in Gas-Injected Leaves[1][OPEN]

Uri Hochberg,[a,b,2] Alexandre Ponomarenko,[a] Yong-Jiang Zhang,[a,c] Fulton E. Rockwell,[a] and N. Michele Holbrook[a,3]

[a]Department of Organismic and Evolutionary Biology, Harvard University, Cambridge, Massachusetts 02138
[b]ARO Volcani Center, Institute of Soil, Water and Environmental Sciences, Bet Dagan, 7505101 Israel
[c]School of Biology and Ecology, University of Maine, Orono, Maine 04469

ORCID IDs: 0000-0002-7649-7004 (U.H.); 0000-0001-5637-3015 (Y.Z.); 0000-0002-2527-6033 (F.E.R.).

Because the xylem in leaves is thought to be at the greatest risk of cavitation, reliable and efficient methods to characterize leaf xylem vulnerability are of interest. We report a method to generate leaf xylem vulnerability curves (VCs) by gas injection. Using optical light transmission, we visualized embolism propagation in grapevine (*Vitis vinifera*) and red oak (*Quercus rubra*) leaves injected with positive gas pressure. This resulted in a rapid, stepwise reduction of transmitted light, identical to that observed during leaf dehydration, confirming that the optical method detects gas bubbles and provides insights into the air-seeding hypothesis. In red oak, xylem VCs generated using gas injection were similar to those generated using bench dehydration, but indicated 50% loss of conductivity at lower tension (~0.4 MPa) in grapevine. In determining VC, this method eliminates the need to ascertain xylem tension, thus avoiding potential errors in water potential estimations. It is also much faster (1 h per VC). However, severing the petiole and applying high-pressure gas could affect air-seeding and the generated VC. We discuss potential artifacts arising from gas injection and recommend comparison of this method with a more standard procedure before it is assumed to be suitable for a given species.

Leaves are widely thought to contain xylem at greatest risk of cavitation, either because of intrinsically vulnerable conduits or the fact that they are exposed to the greatest tensions (Tyree and Ewers, 1991). Reliable and efficient methods to characterize the vulnerability of leaf xylem are thus of substantial interest. This is especially true because rehydration kinetics and evaporative flux, the principal hydraulic methods for evaluating leaf vulnerability, do not distinguish the role of embolism from the extra-xylary pathways in the decline of leaf hydraulic conductance with leaf water potential (Brodribb and Holbrook, 2006; Scoffoni et al., 2017). Novel methodologies such as microcomputed tomography and the optical vulnerability (OV) technique enable visualization of gas propagation, and thus direct measurement of embolism formation (Brodribb et al., 2016b; Scoffoni and Jansen, 2016). Due to its simplicity and low cost, the optical vulnerability technique has been widely adopted to measure embolism propagation in many species (Brodribb et al., 2017; Hochberg et al., 2017; Skelton et al., 2017, 2018). Still, one shortcoming of this method is the long time (several days) required to develop the critical tensions needed for xylem cavitation in intact plants. In addition, the possibility that other dehydration-related processes (shrinkage, cell water content) could alter light interaction with the leaf and appear as cavitation has not been tested.

The optical technique provides valuable information on the temporal and spatial dynamics of gas propagation in leaves (Brodribb et al., 2016a). However, we lack comprehensive understanding of the mechanisms driving this phenomenon. According to the air-seeding hypothesis, gas propagates into a xylem element from its neighbor through intervessel pits. Each pit can withhold a certain pressure difference (ΔP), depending on its membrane chemical composition and structure as well as the overall pit geometry. Once the critical ΔP is surpassed, gas propagates from the adjacent xylem element and cavitation occurs. Under natural conditions, the gas in the xylem is under atmospheric pressure and ΔP is determined by the xylem tension (i.e. negative pressure; Ψ_x). If the air-seeding hypothesis is correct, similar cavitation patterns should occur when the

[1]This work was supported by the Vaadia BARD post-doctoral fellowship (FI-522-2015 to U.H.); the MRSEC (Materials Research Science and Engineering Center at Harvard University; grant no. DMR 14-20570 to A.P.); the National Science Foundation (NSF) (IOS-1456836 to F.E.R.); and the DOD | Air Force Office of Scientific Research (AFOSR) (FA9550-09-1-0188) and the National Science Foundation (NSF) (IOS-1659918) (both to N.M.H.).

[2]Author for contact: hochberg@agri.volcani.gov.il.
[3]Senior author.
The author responsible for distribution of materials integral to the findings presented in this article in accordance with the policy described in the Instructions for Authors (www.plantphysiol.org) is: Uri Hochberg (hochberg@agri.volcani.gov.il).

U.H., F.E.R., and N.M.H. conceived the experiment; U.H., A.P., and F.E.R. took gas injection measurements; Y.-J.Z. took hydraulic measurements; U.H. wrote the manuscript with major contributions from all authors.
[OPEN]Articles can be viewed without a subscription.
www.plantphysiol.org/cgi/doi/10.1104/pp.18.01284

liquid phase is under atmospheric pressure and the gas phase is under positive pressure. Accordingly, Cochard et al. (1992) showed that injecting gas at high pressure into water saturated shoots (i.e. the liquid phase is at atmospheric pressure) resulted in similar loss of conductivity to shoots that were bench dehydrated. This method (Cochard et al., 1992) allowed for fast construction of xylem vulnerability curves (VCs) and helped establish air-seeding as the dominant paradigm for gas propagation through the xylem. Yet, other mechanisms, such as heterogeneous nucleation on imperfectly wettable or hydrophobic surfaces (Pickard, 1981), or the presence of nano-bubbles in the xylem (Schenk et al., 2015), have been suggested as alternative explanations.

As shown in the current paper, we injected gas into leaves (of grapevine, *Vitis vinifera*, and of red oak, *Quercus rubra*) through petioles to visualize embolism propagation using the optical method. We hypothesized that pushing gas into a leaf will result in a similar optical effect to that observed through drying, showing that the change in light transmission captured by the optical method is generated by xylem cavitation. Additionally, we compared the VCs generated by gas injection to those generated through slow dehydration using the optical method (Brodribb et al., 2016b) or, for petioles, the classic hydraulic method (Sperry et al., 1988) to test the centrality of the air-seeding mechanism and the applicability of gas injection into leaves as a rapid method for construction of VCs.

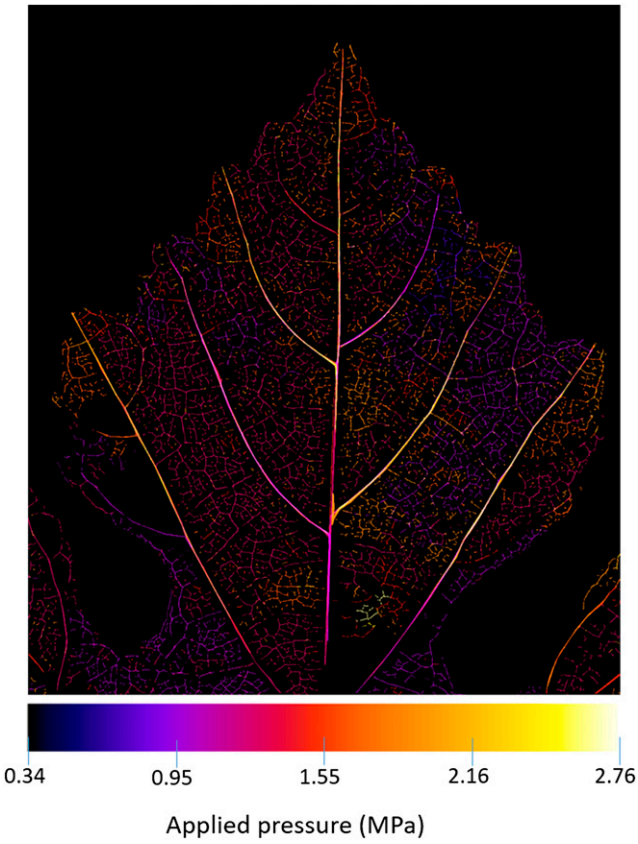

Figure 1. Spatial distribution of the appearance of embolism in a grapevine leaf under positive gas pressure. Cavitation events are colored according to the corresponding injection pressure. For a detailed presentation of embolism propagation see Supplemental Movie S1.

RESULTS

Injecting grapevine or red oak leaves with gas at positive pressure resulted in a stepwise reduction of transmitted light as the injection pressure was increased, paralleling the phenomenon observed when leaves are dried beyond their cavitation threshold (Brodribb et al., 2016b). The spatial pattern of gas propagation was also similar to that observed under dehydration. Generally, cavitation events were first observed in the midrib, propagating onward into minor veins (Figs. 1 and 2; Supplemental Movies S1 and S2). All xylem elements within an areole tended to embolize at similar injection pressures (Supplemental Movies S3 and S4; same as found in Brodribb et al., 2016b; Hochberg et al., 2017).

Despite their similarities, there is an important difference between gas injection and bench drying. When leaves were left under constant pressure for long periods (2 h), cavitation events continued to occur, resulting in an up to 50% increase in cavitated pixels 2 h after the initial increase in pressure (example in Fig. 3). About half of that increase occurred in the first minute after the pressure was set, and most of it in the next 10 min. Still, some cavitation events took place even 2 h after the initial pressure increase. This raises several questions regarding this method, discussed below. It also highlights that using high pressure to achieve seed cavitation is not a perfect analog to native air-seeding under tension. From a methodological perspective, these results demonstrate that gas pressure should be applied for a constant time (in this experiment we used 3 min) when constructing VCs.

The normalized number of pixels showing reduction in gray values was plotted against the gas injection pressure, forming xylem VCs that agreed, in many respects, to VCs established through bench dehydration (Fig. 4; Table 1). The optical method indicated significantly higher vulnerability for grapevine compared with red oak, when embolism was induced either through tension (bench dehydration) or pressure (gas injection). Comparing the two approaches showed similarity in Ψ_{50} values generated through air injection or dehydration for red oak ($\Psi_{50} = -3.38$ or -3.08 MPa, respectively; $n = 4$; $P = 0.34$), but in grapevine, pressurization resulted in significantly ($P = 0.02$) more vulnerable curves compared with dehydration ($\Psi_{50} = -1.34$ for air injection compared with $\Psi_{50} = -1.84$ MPa for dehydration). In both species, pressurization of leaves resulted in higher embolism degree (up to 20%) under low pressure (<1 MPa for grapevine or <2 MPa for red oak) compared with drying leaves that showed no embolism at all under the same (though negative) values (> −1 MPa for grapevine or > −2 MPa for red

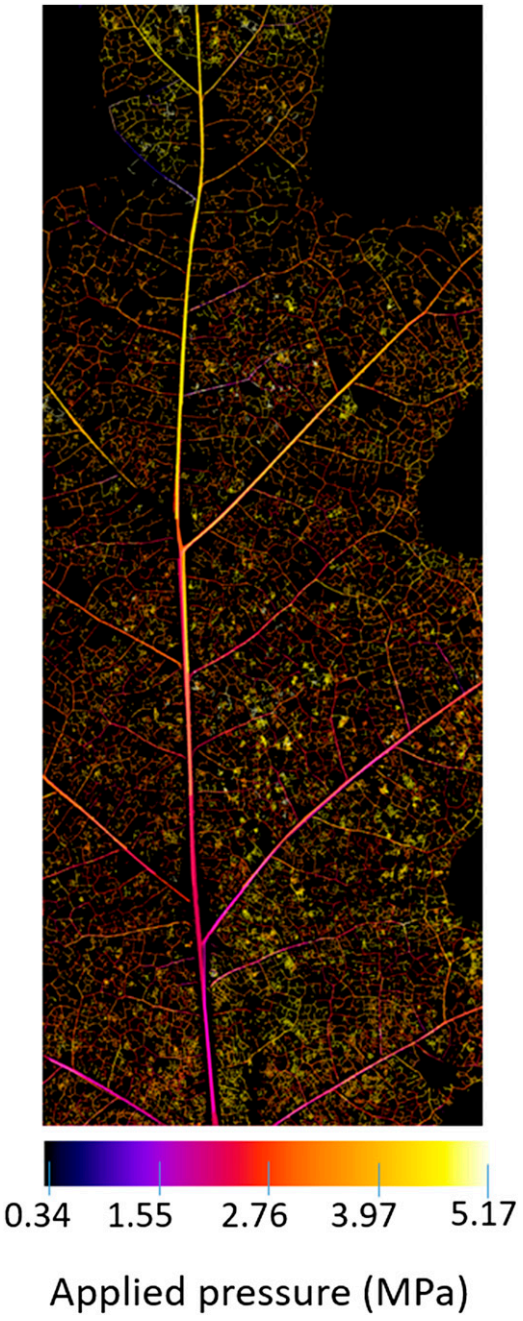

Figure 2. Spatial distribution of the appearance of embolism in a red oak leaf under positive gas pressure. Cavitation events are colored according to the corresponding injection pressure. For a detailed presentation of embolism propagation see Supplemental Movie S2.

oak). Based on measurements using a hydraulic apparatus, the water potential leading to 50% loss of conductance (Ψ_{50}) of petioles was −1.56 MPa for grapevine and −2.77 MPa for red oak.

Finally, we compared two image analysis methods: quantifying the embolism degree using (1) the number of cavitated pixels in the whole leaf detected through images difference analysis (Brodribb et al., 2016b) or (2)

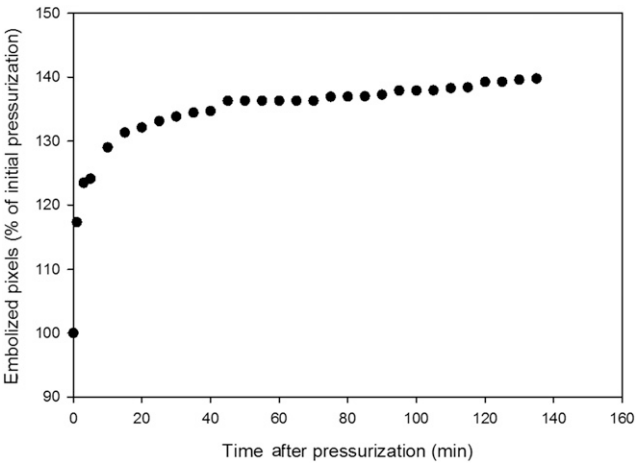

Figure 3. Cavitation events as a function of time since the application of high pressure (2.75 MPa) in a red oak leaf.

the normalized change in gray values in the midrib (assuming gray values before injection is 0% embolism and gray values at the highest pressure is 100% embolism). The first method requires manual 'noise cleaning' and thus can take several hours for each VC, whereas the latter is completely automatic and takes only a couple of minutes. The two methods resulted in nearly identical results (slope = 0.98; r^2 = 0.99; Fig. 5B), suggesting that midrib gray values normalization could provide faster, yet reliable, evaluation of VCs.

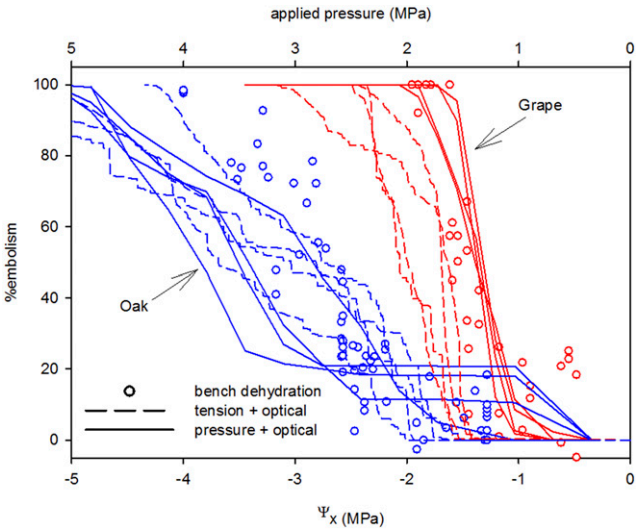

Figure 4. Comparison of vulnerability curves for grapevine (red) and red oak (blue) leaves or petioles, established using three different methods: bench dehydration combined with hydraulic measurements of petioles (Sperry et al., 1988; white circles); the optical method for leaves under tension (Brodribb et al., 2016b; dashed lines); and gas pressure combined with the optical technique for leaves (pressure + optical; black lines).

Table 1. *The water potential leading to 50% loss of conductance (Ψ_{50}; MPa) evaluated using three different methods: bench dehydration in combination with hydraulic measurements (Sperry et al., 1988) of petioles, optical measurement of dehydrating leaves, or gas injection in combination with optical measurement.*

Letters (a, b, c) present statistical difference for methods within the same species.

Mode of Cavitation and Vulnerability Evaluation	Red Oak Ψ_{50}	Grapevine Ψ_{50}
Tension + hydraulic (petioles)	−2.77 ± 0.03 a	−1.56 ± 0.02 b
Tension + optical (leaf veins)	−3.08 ± 0.21 a	−1.84 ± 0.11 a
Pressure + optical (leaf veins)	−3.38 ± 0.21 a	−1.34 ± 0.01 c

DISCUSSION

Centrality of the Air-Seeding Mechanism

Comparing cavitation sourced from gas injection or dehydration supports the centrality and spatial nature of 'air-seeding' in leaves. The similar xylem vulnerability curves achieved by gas injection and dehydration place air-seeding as the major mechanism for xylem cavitation, because none of the other proposed mechanisms (hydrophobic surfaces or nanobubbles; Pickard, 1981; Schenk et al., 2015) could have taken place in the absence of tension. In support, Ponomarenko et al. (2014) used a high-speed camera to observe cavitation propagation in dehydrating wood, showing that cavitation occurred in conduits that neighbored gas and concluding that heterogeneous nucleation is rare relative to the propagation of embolism by air-seeding. The similar spatial propagation between air injection and dehydration (from the midrib onward to minor veins; Supplemental Movies S1–4) suggests that the 'air seed' source is most likely in the midrib, possibly in the form of protoxylem lacuna. These lacunae are a probable source of gas propagation into the xylem network through shared pits between metaxylem and protoxylem (Lens et al., 2013; Rockwell et al., 2014). Their absence in minor veins (Russin and Evert, 1984; Zhang et al., 2016) could explain the spatial pattern observed in dehydrating leaves. Additionally, the few embolized vessels that are naturally present in the midrib even under low tension could be the 'air seed' source (Scoffoni et al., 2017).

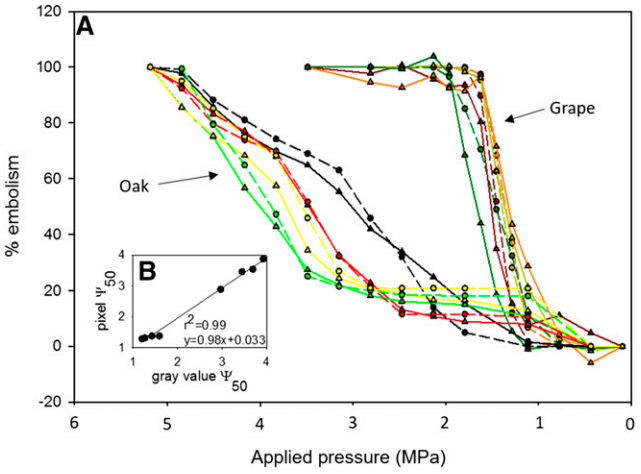

Figure 5. Comparison of two image analysis methods. A, The different colors represent eight different leaves (four red oak and four grapevine) analyzed with either gray value normalization (dashed lines and circles) or pixel normalization (solid lines and triangles). B, The regression between the gas injection pressure that led to 50% embolism using the two methods.

Potential for a New Method

The results provide strong support for the validity of the optical method (Brodribb et al., 2016b). The similar optical phenomenon that was observed when leaves were dehydrating or injected with gas suggest that the signal indeed results from gas propagation through the xylem, rather than other drought-related processes (air-injected leaves were protected from water loss). The optical method was already shown to yield similar Ψ_{50} to those acquired through rehydration kinetics measurements in four species (Brodribb et al., 2016b), and recently gained additional support from comparison of VCs constructed for stems using the optical technique and the cavitron in many species (Brodribb et al., 2017). The current results show similar VCs for the optical technique and classic bench dehydration of petioles, providing further support for the validity of the method. Because the optical method allows affordable visualization of intact plants, its popularity is likely to grow in the coming years, providing a large database of xylem vulnerability data (http://www.opensourceov.org).

Combining the optical method with gas injection into leaves has the potential for becoming a reliable high throughput method for determining leaf xylem vulnerability, allowing the xylem vulnerability database to be expanded further. When applied to red oak leaves, the method produced comparable results to the optical method applied to dehydrating leaves, and also to petioles measured with hydraulic apparatus. Air injection has two major advantages over other methods designed for leaves. First, there is no need to determine Ψ_l, which is an advantage because under cavitation conditions, both pressure chamber and stem psychrometer estimations of Ψ_l have limitations (Charrier et al., 2016). Second, it is much faster—1 h per curve compared with days using other methods.

Although these advantages present the method as a promising tool to investigate xylem vulnerability, the

difference between grapevine VCs generated using gas injection and dehydration (Fig. 4), as well as the continuous cavitation events that were observed even 2 h after the pressure was increased (Fig. 3), highlight several important concerns to be considered:

(1) The gas-to-liquid pressure difference is equal to the air injection pressure ($\Delta P = P_{inj}$) only when Ψ_x is zero

Full hydration before air injection and elimination of transpiration should prevent Ψx from becoming negative. However, the water released from cavitated vessels could create positive pressure in liquid-filled vessels, thus creating a scenario where $\Delta P <$ PinJ. In grapevine, guttation was apparent during the injection, secreting excessive water and preventing pressure increase of the liquid phase. No guttation was observed in red oak leaves, possibly resulting in flooding of intercellular air spaces or xylem sap pressure increase.

(2) Severing the petiole could place many xylem vessels that were not formerly in contact with gas in danger of air-seeding

With the assumption that xylem cavitation is a function of gas propagation from neighboring vessels (air-seeding hypothesis), introducing air into the midrib upon cutting the petiole and, in the case of long vessel species such as grapevine and red oak, also into higher vein orders (Chatelet et al., 2006), could result in a more vulnerable xylem compared with intact leaves. This could explain the highly vulnerable vessels that cavitated in remote parts of the leaf (Supplemental Figs. S1 and S2). Furthermore, the long vessels that were severed upon cutting cannot be measured for vulnerability. If these long vessels in the midrib are more vulnerable than the other vessels in the leaf (Brodribb et al., 2016a), their exclusion will result in a more resistant VC than the real one.

(3) Mechanical damage associated with high-pressure injection could lead to leaks

Even when the petiole connection is perfectly sealed, the applied pressure could damage xylem elements, resulting in unavoidable leakages. Loud breaking sounds were evident when injecting both species: red oak at ~4 MPa and grapevine at ~1.75 MPa. Additionally, in most of the grapevine leaves (3 out of 4), up to 20% of the total leaf area was completely uncavitated (Supplemental Fig. S1), possibly as leakage prevented gas pressure from reaching these regions. The uncavitated area included both major and minor veins.

(4) Exposing the xylem sap to high-pressure gas could alter its surface tension because of adsorption of gas at the liquid surface

For N_2 (used in this experiment) at 6 MPa, Massoudi and King (1974) measured 5% reduction in water surface tension, suggesting a minor effect on the air injection values reported here. However, it is important to mention that other gases could have a substantially larger effect (Massoudi and King, 1974; Luijten et al., 1997). Additionally, following Henry's law, at high pressure, gas will dissolve into the liquid and could diffuse into nearby gas pockets, increasing their pressure to further propagate embolism.

5) The pressure in air-seeded vessels is not necessarily equal to P_{inj}

Air-seeding of the pit membrane is thought to occur as a snap-off event (Roof, 1970), meaning that there is no gas continuity between two cavitated vessels (Jansen et al., 2018). Instead, the pressure in the newly air-filled vessel will increase to P_{inj} minus the critical ΔP needed for cavitation. From that point onward, both the ΔP from the source conduit to the newly air-seeded conduit and the ΔP from that conduit to the next conduit in series are smaller than the critical ΔP needed for cavitation. Gas movement into the newly embolized conduit will be only by diffusion across the pit membranes. Although this could lead to the pressure in the embolized conduit rising to P_{inj} within seconds to minutes, we expect that diffusive losses to surrounding conduits that are not saturated with gas, and ultimately to the atmosphere, will prevent equilibration of the embolized conduit gas pressure with P_{inj}. This mechanism explains the positive correlation between the stem length and the air seed pressure required to embolize stems injected from one end (Christman et al., 2009).

By contrast, in drying plants where the xylem is under tension and P_{inj} equals atmospheric pressure, diffusion of gas from the surrounding conduits (whether filled with gas or liquid saturated with gas at atmospheric pressure) should rapidly bring a newly embolized conduit to atmospheric pressure (Wang et al., 2015), and the next conduit in the series will again be tested at the critical ΔP of the previous air-seeding event (assuming the water released by cavitation is small in volume compared with the capacitance of the system, and so does not relax the tension).

Because the behavior of capillary seals in series is well understood in fluid dynamics (Singh et al., 2017), but less so in plant hydraulics, we illustrate it with a simple study of air-seeding in a system of two filters (0.2 μm) in series (Supplemental Movies S5 and S6). For clarification, the empty pipe coming down from the three-way valve in the two filters movie is connected to the pressure gauge on the left (Supplemental Movies S5 and S6). Air-seeding the first filter resulted in many small bubbles, attesting to snap-off events as the mode of failure. After air-seeding the first filter (at 50 PSI), as p_{inj} was increased, the pressure in between the filters reached a value that is lower than P_{inj} by 50 PSI (the critical ΔP; Supplemental Movie S5). Air-seeding the second filter in this system required bringing the pressure applied at the first filter to a value just over 100 PSI, which resulted in 50 PSI in between the two filters. These results

are also summarized in https://www.youtube.com/watch?v=KApK5tdL1rc. Maintaining P_{inj} at 55 PSI led to an increase of the pressure between the filters to 35 PSI over 8 h, and then to 37 to 38 PSI after 23 h, with no further increase over the next 4 h (Supplemental Movie S6). The slow rise in gas pressure to a steady value below P_{inj} is consistent with the evolution of the gas pressure between the filters to a value representing the balance between diffusive gain and loss. Similar diffusive effects could explain the continuous appearance of cavitation events in our leaf air injection experiments when the pressure was set to a constant value (as in Fig. 3 or in the results of Yin and Cai, 2018).

The filters-in-series system (Supplemental Movies S5 and S6) suggests that VCs acquired using positive gas pressures compared with those achieved by negative pressure in the liquid phase are not equivalent for systems of two or more membranes in series; thus we should not necessarily expect agreement between air injection and bench drying. However, our results with grapevine and red oak showed reasonable agreement (<0.4 MPa difference in ψ_{50}) between gas injection and dehydration. A possible explanation for this agreement is that both species have long vessels and thus fewer pits in series. However, we cannot rule out the possibility that structural and compositional differences between the pores in cellulose filters versus pit membranes (Herbette and Cochard, 2010; Herbette et al., 2015; Pereira et al., 2018) may lead to different modes of failure (Rockwell et al., 2014). We urge caution in extrapolating apparent agreement between air injection and bench drying methods for particular taxa and sample characteristics (i.e. length, [Ennajeh et al., 2011]) as a general validation of this method.

Despite rapid image acquisition when cavitation is seeded with gas pressure, the subsequent image analysis can require substantial amounts of time (hours per curve) depending on image quality, movement of the leaf during acquisition, and leaf characteristics. The similar results acquired through both image analysis methods (Fig. 5) suggest that using the gray value normalization approach is a valid procedure to establish a vulnerability curve. The method resulted in a slightly more vulnerable VC (slope = 0.98; Fig. 5B), probably owing to the fact that minor veins, which are typically less vulnerable (Brodribb et al., 2016a), are excluded from the gray value analysis. The gray value processing method takes only a few minutes per curve and requires no human intervention, thus preventing bias. Using the same approach to analyze dehydrating samples is tempting, but might prove difficult because the dehydration process itself (leaf shrinkage, water content, etc.) will also affect light transmission.

In conclusion, the findings of this study confirm that the optical method (Brodribb et al., 2016b) detects gas bubbles and implicates air-seeding as the major mechanism for xylem cavitation. A combination of gas injection with the optical method has the potential of becoming a high throughput method for checking the xylem vulnerability of leaves. Having said that, concerns arising from severing the xylem or applying high gas pressure require that it be compared with more standard methods before it can be assumed suitable for new species.

MATERIALS AND METHODS

All experiments were performed on two species: grapevine (*Vitis vinifera*) and red oak (*Quercus rubra*). For grapevine, we used fully irrigated 3-year-old Chardonnay vines planted in 7 L pots. Vines were grown under a controlled environment with day/night cycles of 14/10 h and temperatures of 25°/20°C, respectively. Light intensity was 400 μmol m^{-2} $s^{-1.}$ and relative humidity was between 50% and 75%. For oak we used mature irrigated red oak trees growing on the campus of the Harvard Divinity School. Sun-exposed branches were collected between August and September with a pole pruner.

Xylem Vulnerability of Petioles-Hydraulic Method

Long shoot segments (1.5 m) were bench-dehydrated to a range of xylem potentials. Shoots were covered with black plastic bags for at least 20 min to equilibrate the leaf and stem water potentials, before Ψ_x of two leaves per shoot was measured using a pressure chamber (Soil Moisture Equipment Inc.). Petioles were harvested under water after tension was relaxed (10 min relaxation; as explored in Wheeler et al., 2013; Hochberg et al., 2016), and their percent loss of hydraulic conductivity (PLC) was measured with Sperry-type apparatus (Sperry et al., 1988). The cut ends of the petiole were connected to tubing, and flow rates were monitored using a precision balance (Sartorius CPA225D, Göttingen) connected to a computer. Flow passing through the petiole section was generated by a 5-cm-high pressure head, with filtered (0.2 μm) 20 mmol KCl solution used as the perfusion fluid. To reach the maximum conductance of a measured sample, petioles were flushed for 3 min with a pressure head of 150 kPa, after which the flow direction was reversed and the sample flushed again for another 3 minutes. To calculate the Ψ_l that corresponds with 50% PLC (Ψ_{50}), the relationship between water potential and conductance was fit to a sigmoidal regression:

$$PLC = \frac{100}{1 + e^{\alpha(\psi_x - \psi_{50})}}$$

Embolism Propagation in Drying Leaves

Embolism spread was evaluated following the method of Brodribb et al. (2016b), in which embolism is detected by monitoring changes in light transmission through leaf venation (Mayr et al., 2014; Ponomarenko et al., 2014). Four shoots (1.5 m length) from each species were dried for 2 (grapevine) or 6 (red oak) days while one of their leaves was imaged. The adaxial side of the leaf was fixed to the microscope surface using transparent double-sided tape, leaving the stomata uncovered. Leaves were imaged with a light microscope under 7.5× magnification (M80, Leica Microsystems) every 2 min (grapevine) or 5 min (red oak). The leaf was continuously illuminated from below to create an image of transmitted light, which was recorded by a digital camera (DFC290, Leica Microsystems). The imaged area of 17 × 10 mm encompassed all vein orders including the midrib; each image consisted of 1920 × 1080 pixels, resulting in an 8.8 μm/pixel resolution. Leaf water potential (Ψ_l) of other leaves from the same shoot was measured every 1 to 5 h using a pressure chamber (Soil Moisture Equipment Inc.) resulting in a ~0.2 MPa interval between Ψ_l measurements. Ψ_l was interpolated to the entire dehydration period using the best fit Ψ_l versus time regression.

Air Injection into Leaves

To examine the propagation of gas in the xylem under positive pressure, leaves were scanned while being injected with increasing pressures. The petiole was cut under water and connected to tubing with water, at least 30 min before scanning and until right before injection commenced. At the same time the leaf was covered with a plastic bag to achieve xylem potential near atmospheric (i.e. $\Psi_x = 0$). Then, the adaxial side of the leaf was fixed to the scanner (CanonScan 9000F MarkII) surface using transparent double-sided tape. The leaf was also taped from its abaxial side so that it was completely covered to further decrease its movement and prevent water loss during the scan. Just before scanning, the petiole was removed from the water filled tubing and connected to a

high-pressure nitrogen source. The petiole was connected via a compression fitting (B-200-6, with the ferrule replaced by two O-rings; Swagelock) to 1/8 inch Poly ether ether ketone tubing (51085K49, McMaster-Carr) connected to a Scholander pressure chamber (Soil Moisture Equipment). To prevent dehydration of the leaf with time, the scanner was filled with wet paper towels, the nitrogen was humidified by passing it through water, and the scanner lid was sealed with tape to the scanner surface. The leaf was scanned (transmitted light scanning) one time under atmospheric pressure and then at step increases of pressure (each step was 0.17 to 0.7 MPa) in accordance with the expected xylem vulnerability. Pressure was increased at a rate of 2 PSI/s, and scans were acquired 3 minutes after the desired injection pressure (P_{inj}) was reached. Because each pressure increase led to small movements of the petiole and the blade near the petiole (taping the petiole proved difficult due to the pressure fitting), only the distal part of the leaf was imaged (as indicated in Supplemental Fig. S1). The imaged area was 15–25 cm^2 with a resolution of 21.3 μm/pixel.

Image Analysis for the Detection of Embolism

Image analysis was performed as described in Hochberg et al. (2017) using a custom algorithm executed in ImageJ (https://imagej.nih.gov/ij/). Consecutive images were subtracted to produce a set of difference images in which white pixels represent any optical event: cavitation, instability of light conditions, and movements of the leaf, a trichome, or a bug. To separate the signal (cavitation event) from noise, the difference images were processed according to the following sequence: a brightness increase (25%), a median filtering using 3×3 neighboring pixels, a threshold adjustment (8%), and a second median filtering. The resulting images typically contain some degree of noise, normally originating from movement of trichomes or bugs, which therefore bear their shape. All images were carefully examined, and the remaining noise was manually removed. The degree of embolism (%emb) was calculated as the cumulative number of embolized pixels normalized to the total number of embolized pixels throughout the dehydration. Finally, to visualize the dynamics of embolism spread through the leaf, events were colored on a continuous scale with respect to the time at which they appeared. Analysis of two consecutive images can take up to 3 min (when there is lots of cavitation events and lots of noise) and a whole imaging sequence of a dehydrating leaf up to 5 h (depending on the number of images and noise level).

To reduce the image analysis time, we tested an alternative approach for all air-injected leaves. The analysis was performed using ImageJ. A ~400 pixel polygon containing only the midrib was marked in the center of the image. The gray values of this polygon were measured automatically for all the images (each taken at a different injection pressure) using the 'plot z-axis profile' command. The gray values were normalized into a vulnerability curve so that the first image represent 0% embolism and the last 100% embolism. Because the leaf was completely covered during air injection, it is reasonable to assume that all changes in light transmittance resulted from gas embolism (rather than the dehydration and shrinkage of cells that could also change optical density). It is important to note that unlike minor veins, the midrib contains a large pool of xylem vessels, and their gradual cavitation could be normalized across a vulnerability curve. A technical explanation on constructing a normalized gray value VC is available in Supplemental Movie S7.

SUPPLEMENTAL DATA

The following supplemental materials are available:

Supplemental Figure S1. Example for areoles with no cavitation in grapevine leaves subjected to gas pressure.

Supplemental Movie S1. Spatial distribution of embolism appearance in a grapevine leaf under positive gas pressure.

Supplemental Movie S2. Spatial distribution of embolism appearance in an red oak leaf under positive gas pressure.

Supplemental Movie S3. A time-lapse of embolism propagation in a grapevine leaf imaged with a microscope during 28 h after it was disconnected from its roots.

Supplemental Movie S4. A time lapse of embolism propagation in an red oak leaf imaged with a microscope during 100 h after a long branch was cut and left to dry.

Supplemental Movie S5. A gradual pressure increase in two membranes in series configuration.

Supplemental Movie S6. Holding a constant pressure in two membranes in series configuration.

Supplemental Movie S7. An explanation of how to construct a vulnerability curve from an image sequence using gray value normalization.

Received October 18, 2018; accepted February 20, 2019; published March 6, 2019.

LITERATURE CITED

Brodribb TJ, Holbrook NM (2006) Declining hydraulic efficiency as transpiring leaves desiccate: Two types of response. Plant Cell Environ **29:** 2205–2215

Brodribb TJ, Bienaimé D, Marmottant P (2016a) Revealing catastrophic failure of leaf networks under stress. Proc Natl Acad Sci USA **113:** 4865–4869

Brodribb TJ, Skelton RP, McAdam SA, Bienaimé D, Lucani CJ, Marmottant P (2016b) Visual quantification of embolism reveals leaf vulnerability to hydraulic failure. New Phytol **209:** 1403–1409

Brodribb TJ, Carriqui M, Delzon S, Lucani C (2017) Optical measurement of stem xylem vulnerability. Plant Physiol **174:** 2054–2061

Charrier G, Torres-Ruiz JM, Badel E, Burlett R, Choat B, Cochard H, Delmas CE, Domec J, Jansen S, King A (2016) Evidence for hydraulic vulnerability segmentation and lack of xylem refilling under tension. Plant Physiol **172:** 1657–1668

Chatelet DS, Matthews MA, Rost TL (2006) Xylem structure and connectivity in grapevine (*Vitis vinifera*) shoots provides a passive mechanism for the spread of bacteria in grape plants. Ann Bot **98:** 483–494

Christman MA, Sperry JS, Adler FR (2009) Testing the 'rare pit' hypothesis for xylem cavitation resistance in three species of Acer. New Phytol **182:** 664–674

Cochard H, Cruiziat P, Tyree MT (1992) Use of positive pressures to establish vulnerability curves: Further support for the air-seeding hypothesis and implications for pressure-volume analysis. Plant Physiol **100:** 205–209

Ennajeh M, Nouiri M, Khemira H, Cochard H (2011) Improvement to the air-injection technique to estimate xylem vulnerability to cavitation. Trees (Berl) **25:** 705–710

Herbette S, Cochard H (2010) Calcium is a major determinant of xylem vulnerability to cavitation. Plant Physiol **153:** 1932–1939

Herbette S, Bouchet B, Brunel N, Bonnin E, Cochard H, Guillon F (2015) Immunolabelling of intervessel pits for polysaccharides and lignin helps in understanding their hydraulic properties in *Populus tremula* × *alba*. Ann Bot **115:** 187–199

Hochberg U, Herrera JC, Cochard H, Badel E (2016) Short-time xylem relaxation results in reliable quantification of embolism in grapevine petioles and sheds new light on their hydraulic strategy. Tree Physiol **36:** 748–755

Hochberg U, Windt CW, Ponomarenko A, Zhang YJ, Gersony J, Rockwell FE, Holbrook NM (2017) Stomatal closure, basal leaf embolism, and shedding protect the hydraulic integrity of grape stems. Plant Physiol **174:** 764–775

Jansen S, Klepsch MM, Li S, Kotowska MM, Schiele S, Zhang Y, Schenk HJ (2018) Challenges in understanding air-seeding in angiosperm xylem. Acta Hortic **1222:** 13–20

Lens F, Tixier A, Cochard H, Sperry JS, Jansen S, Herbette S (2013) Embolism resistance as a key mechanism to understand adaptive plant strategies. Curr Opin Plant Biol **16:** 287–292

Luijten C, Bosschaart K, Van Dongen M (1997) High pressure nucleation in water/nitrogen systems. J Chem Phys **106:** 8116–8123

Massoudi R, King A, Jr. (1974) Effect of pressure on the surface tension of water. Adsorption of low molecular weight gases on water at 25. deg. J Phys Chem **78:** 2262–2266

Mayr S, Kartusch B, Kikuta S (2014) Evidence for air-seeding: watching the formation of embolism in conifer xylem. J Plant Hydraul **1:** e0004

Pereira L, Flores-Borges DNA, Bittencourt PRL, Mayer JLS, Kiyota E, Araújo P, Jansen S, Freitas RO, Oliveira RS, Mazzafera P (2018) Infrared nanospectroscopy reveals the chemical nature of pit membranes

in water-conducting cells of the plant xylem. Plant Physiol **177:** 1629–1638

Pickard WF (1981) The ascent of sap in plants. Prog Biophys Mol Biol **37:** 181–229

Ponomarenko A, Vincent O, Pietriga A, Cochard H, Badel É, Marmottant P (2014) Ultrasonic emissions reveal individual cavitation bubbles in water-stressed wood. J R Soc Interface **11:** 20140480

Rockwell FE, Wheeler JK, Holbrook NM (2014) Cavitation and its discontents: Opportunities for resolving current controversies. Plant Physiol **164:** 1649–1660

Roof J (1970) Snap-off of oil droplets in water-wet pores. Soc Pet Eng J **10:** 85–90

Russin WA, Evert RF (1984) Studies on the leaf of *Populus deltoides* (Salicaceae): Morphology and anatomy. Am J Bot **71:** 1398–1415

Schenk HJ, Steppe K, Jansen S (2015) Nanobubbles: A new paradigm for air-seeding in xylem. Trends Plant Sci **20:** 199–205

Scoffoni C, Jansen S (2016) I can see clearly now–embolism in leaves. Trends Plant Sci **21:** 723–725

Scoffoni C, Albuquerque C, Brodersen CR, Townes SV, John GP, Bartlett MK, Buckley TN, McElrone AJ, Sack L (2017) Outside-xylem vulnerability, not xylem embolism, controls leaf hydraulic decline during dehydration. Plant Physiol **173:** 1197–1210

Singh K, Menke H, Andrew M, Lin Q, Rau C, Blunt MJ, Bijeljic B (2017) Dynamics of snap-off and pore-filling events during two-phase fluid flow in permeable media. Sci Rep **7:** 5192

Skelton RP, Brodribb TJ, Choat B (2017) Casting light on xylem vulnerability in an herbaceous species reveals a lack of segmentation. New Phytol **214:** 561–569

Skelton RP, Dawson TE, Thompson SE, Shen Y, Weitz AP, Ackerly D (2018) Low vulnerability to xylem embolism in leaves and stems of North American oaks. Plant Physiol **177:** 1066–1077

Sperry J, Donnelly J, Tyree M (1988) A method for measuring hydraulic conductivity and embolism in xylem. Plant Cell Environ **11:** 35–40

Tyree MT, Ewers FW (1991) The hydraulic architecture of trees and other woody plants. New Phytol **119:** 345–360

Wang Y, Liu J, Tyree MT (2015) Stem hydraulic conductivity depends on the pressure at which it is measured and how this dependence can be used to assess the tempo of bubble pressurization in recently cavitated vessels. Plant Physiol **169:** 2597–2607

Wheeler JK, Huggett BA, Tofte AN, Rockwell FE, Holbrook NM (2013) Cutting xylem under tension or supersaturated with gas can generate PLC and the appearance of rapid recovery from embolism. Plant Cell Environ **36:** 1938–1949

Yin P, Cai J (2018) New possible mechanisms of embolism formation when measuring vulnerability curves by air injection in a pressure sleeve. Plant Cell Environ **41:** 1361–1368

Zhang YJ, Rockwell FE, Graham AC, Alexander T, Holbrook NM (2016) Reversible leaf xylem collapse: A potential 'circuit breaker' against cavitation. Plant Physiol **172:** 2262–2274